

Solution-processed cesium carbonate doped electron transport layer for multilayered polymer light emitting devices

MORA VEERA MADHAVA RAO*, CHEOL HEE MOON*

Department of Display Engineering, Hoseo University, Baebang, Chonan, South Korea

Efficient multilayered high yellow polymer light-emitting devices were successfully fabricated using a solution-processed n-doped small molecular electron transporting layer composed of 1,3,5-tris(N-phenyl-benzimidazol-2-yl)-benzene (TPBi) and Cs_2CO_3 . We found that the electroluminescence properties of the devices with Cs_2CO_3 -doped TPBi electron transport layers (ETL) are significantly improved. The maximum luminance efficiency of the device with Cs_2CO_3 doped TPBi ETL reached 6.7 cd/A, which is 20% higher as that of the undoped device. These results demonstrate that Cs_2CO_3 can be used as an effective n-dopant in solution-processed devices.

(Received September 27, 2017; accepted April 5, 2018)

Keywords: Polymer light emitting devices, Electron transport layer, Solution processing, Electroluminescence

1. Introduction

Organic/Polymer light emitting diodes (OLEDs/PLEDs) have received a considerable attention for display and lighting applications due to their wide viewing angle, easy fabrication process and flexibility. The light emission performance of OLEDs depends on several important parameters such as charge balance factor, internal and external quantum efficiencies, and efficient charge carrier injection and transport. Among these, good charge carrier injection without any barrier is always desirable for the high performances of OLEDs [1-6]. The work function difference between the electrode and emissive layer forms an energy barrier for charge injection, which results in poor device performance. One of the possible approaches to improve the light emission performance of OLEDs is by using efficient charge carrier injection layer. Generally, indium-tin-oxide (ITO) is used as an anode in the OLED devices due to their high transmittance and a high work function value with low energy barrier for hole injection. In contrast, the work function of reflective aluminum cathode is not suitable for electron injection. Therefore, various electron injection materials are reported especially inorganic materials such as magnesium (Mg), lithium fluoride (LiF), lithium chloride (LiCl), cesium chloride (CsCl), and which is used for reducing energy barrier between cathode and the electron transport layer. But these materials have disadvantages owing to high deposition temperature, narrow thickness margin, and hard to control deposition process. Instead of these inorganic materials, metal-organic ligand complexes such as lithium 8-quinolate (Liq) and Lithium 2-(2-pyridyl)phenolate (LIPP) are reported for low temperature process, wider thickness process margin, and easily controllable deposition process. Recently several research reports on modified metal-organic ligand

complexes. However, considerable method to design new efficient electron injection complexes for high performance of OLEDs is poorly reported [6-15].

However, the effectiveness of these buffers or electron injection materials is very sensitive to the choice of metal, and only Al has been found to provide good device performance. Similar to inorganic semiconductor electrical doping in organic semiconductors can be an alternative approach to enhance the carrier injection, transport and resulting in enhanced device performance [11-21]. The most widely investigated n-type dopants for the ETL are alkali metals. However, these approaches are difficult because the material is highly reactive to be oxidized and highly diffusive in an organic matrix, which causes the quenching of excitons in the emissive layer [22-30].

However, a vacuum-deposited ultrathin alkali salt buffer layer is usually inserted between solution-processed ETL and cathode to reduce electron-injection barrier. As an alternative approach, n-doping can enhance electron-injection and transport of ETLs. The n-doping of ETL is typically realized by co-evaporating the electron-transport materials with a strong electron donor like Cs_2CO_3 , LiF and LiN_3 [23]. Very recently, n-doping of small molecule electron transport materials by alkali carbonates (Cs_2CO_3 and Li_2CO_3) have been developed by solution-processing [22]. It has been reported that, the n-doped ETLs show considerable reduction in driving voltage and improvement in device efficiency compared to a conventional device [23].

In this work, we present efficient multilayer PLEDs using Cs_2CO_3 as an effective n-dopant for solution-processed ETLs. We found that the solution-processed n-doped ETLs exhibited smooth surface morphology. Incorporation of the dopant into TPBi significantly improved the performances of the devices. The devices exhibit high current efficiencies of 6.7 cd/A (Cs_2CO_3

doped TPBi) which are 20% higher than that of the reference device with undoped (TPBi) ETLs.

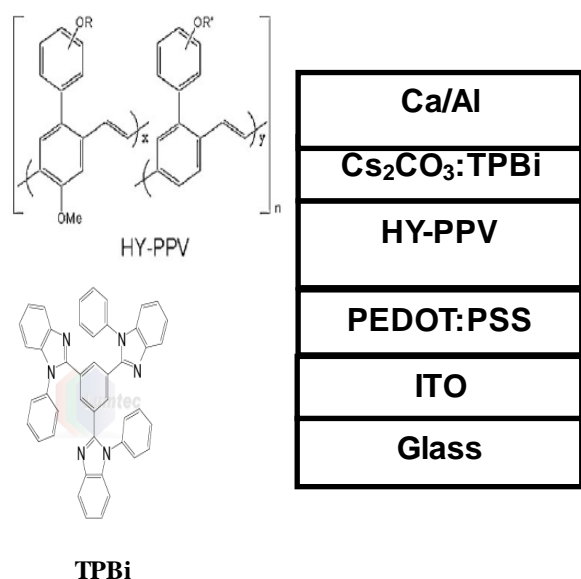


Fig. 1. Chemical structure of the organic materials and a typical device structure of the PLED used in this study

2. Experimental

The Hole-injection material poly(3,4-ethylenedioxythiophene):poly(styrenesulfonate) (PEDOT:PSS, P VP AI 4083) and the yellow-emitting material (High Yellow; HY-PPV) were purchased from H. C. Starck Inc. and Merck respectively. A multilayer PLED, with a structure of glass/ITO/PEDOT:PSS/HY-PPV/TPBi/Ca/Al, was fabricated by subsequent procedures to investigate its optoelectronic characteristics. A glass substrate coated with an ITO conductive layer was successively deposited with PEDOT:PSS as the hole-injection layer, HY-PPV as the emitting layer, TPBi, layer as the electron transporting layer, and calcium and aluminum as the metal cathode. The ITO-coated glass was washed in an ultrasonic bath successively using a neutral detergent water, de-ionized water, acetone and 2-propanol, followed by treatment in a UV-ozone chamber. A thick hole-injection layer of PEDOT:PSS was spin-coated on top of the cleaned ITO glass and annealed at 120 °C for 30 min in a dust-free atmosphere. The emitting layer (EML) was deposited by spin-coating the HY-PPV solution on top of the PEDOT:PSS layer and annealed at 80 °C for 30 min to remove the residual solvent. An electron transport layer of Cs₂CO₃ doped TPBi was spin coated on emissive layer, followed by drying for 30 min 70 °C under an inert atmosphere. Finally, Ca and aluminum were deposited in an evaporation chamber at about 2×10^{-6} Torr with respective thermal-deposition rates of 0.01 nm/s and 0.1 nm/s. For the measurement of device characteristics. Current density-Voltage (I-V) and Brightness-Voltage (B-V) changes were measured using a power supply (Keithley 2400) and a fluorescence spectrophotometer (Ocean optics usb 2000), and the

luminance was further corrected by SpectraScan PR650 spectrophotometer. Current efficiency efficiency was calculated from the I-L-V characteristics curves. The devices were fabricated under ambient conditions with the subsequent optoelectronic measurements conducted in a glove-box filled with nitrogen. The active area of the Electroluminescence (EL) devices by overlapped of the ITO and the cathode electrodes was 6 mm². The device configuration and molecular structure of HY-PPV and TPBi are shown in Fig. 1.

3. Results and discussions

TPBi is widely used as electron transport layer for OLED devices due to its high triplet energy level (2.73 eV) and appropriate lowest unoccupied molecular orbital (LUMO) level (2.7 eV). In addition, TPBi is soluble in the polar solvents, such as formic acid, methanol and ethanol, which facilitates multilayer devices to be fabricated by solution-processing. The film-forming properties of the organic functional layers are important for the devices in connection with their performance [30].

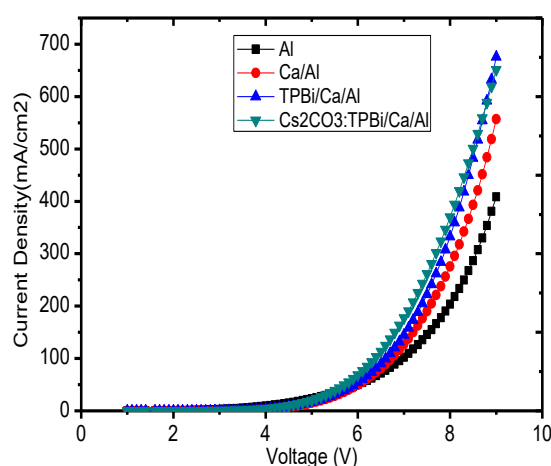


Fig. 2. Current density-Voltage curves of the devices using Al, Ca/Al TPBi/Ca/Al and Cs₂CO₃:TPBi/Ca/Al as the device cathode

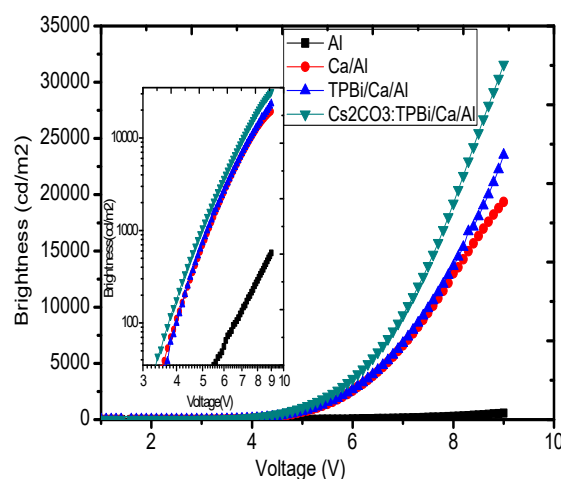


Fig. 3. Brightness-voltage curves of the devices using Al, Ca/Al TPBi/Ca/Al and Cs₂CO₃:TPBi/Ca/Al as the device cathode

Fig. 2 shows the current density-voltage characteristics of the Al cathode, Ca/Al cathode, TPBi/Ca/Al cathode and $\text{Cs}_2\text{CO}_3\text{:TPBi/Ca/Al}$ cathode devices. As the Current density-voltage curves depict that, the TPBi cathode device shows the highest current density while that of the Al cathode device is the lowest. The OLED with the TPBi/Ca/Al cathode and $\text{Cs}_2\text{CO}_3\text{:TPBi/Ca/Al}$ cathode exhibits the I-V characteristics of a diode. The injected current is much higher than that of a device in which Al and Ca/Al are the cathode, at a given bias voltage. This is due to the carrier mobility difference between the electron transport layers, as well as the energy barrier difference between the electron transport layers and emissive layer. Fig. 3 shows that brightness-voltage characteristics of the Al, Ca/Al, TPBi/Ca/Al and $\text{Cs}_2\text{CO}_3\text{:TPBi/Ca/Al}$ cathode devices. The light turn-on voltage is brought forward to 3.3 V for the device with the $\text{Cs}_2\text{CO}_3\text{:TPBi/Ca/Al}$ cathode, which is 5.6 V for the device with the Al cathode (inset of Fig. 3 shows that log-log scale brightness-voltage characteristics). The higher injected current and the forward shift in the light turn-on voltage to the lower bias condition for the device with the $\text{Cs}_2\text{CO}_3\text{:TPBi/Ca/Al}$ cathode are attributable to the improvement in the electron injection through the Al cathode.

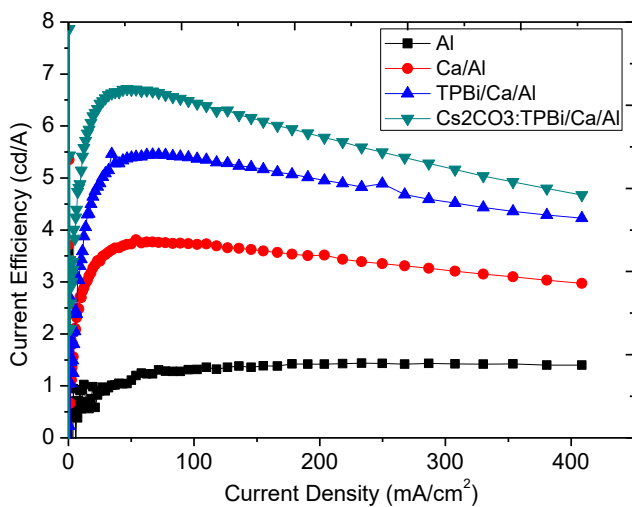


Fig. 4. The current efficiency versus current density for the devices applying Al, Ca/Al/TPBi/Ca/Al and $\text{Cs}_2\text{CO}_3\text{:TPBi/Ca/Al}$ as the device cathode

Fig. 4 shows that current efficiency versus current density of device with an Al cathode, Ca/Al cathode, TPBi/Ca/Al cathode, and $\text{Cs}_2\text{CO}_3\text{:TPBi/Ca/Al}$ cathode. The maximum current efficiency of the device with the $\text{Cs}_2\text{CO}_3\text{:TPBi/Ca/Al}$ cathode is 6.7 cd/A (bias voltage at 6V, 68.31 mA/cm^2 , 3641 cd/m^2), while that of the only Al cathode device is 1.44 cd/A (bias voltage at 8.2V, 233.3 mA/cm^2 , 335.9 cd/m^2), device cathode Ca/Al is 3.8 cd/A (bias voltage at 6.1V, 53.9 mA/cm^2 , 2900 cd/m^2) and TPBi/Ca/Al cathode is 5.45 cd/A (bias voltage is 6.2V, 67.02 mA/cm^2 , 3289 cd/m^2). Polymer light-emitting diodes employing a soluble small molecular materials and Cs_2CO_3 blended interfacial layer as the electron-injection

layer exhibit remarkable enhancement in the performance of solution-processed devices. This simple concept of using the TPBi: Cs_2CO_3 blended interfacial layer could become greatly attractive in the future when large area PLEDs are fabricated under atmospheric pressure. This work is thus anticipated to be helpful and valuable for the development of solution processed devices.

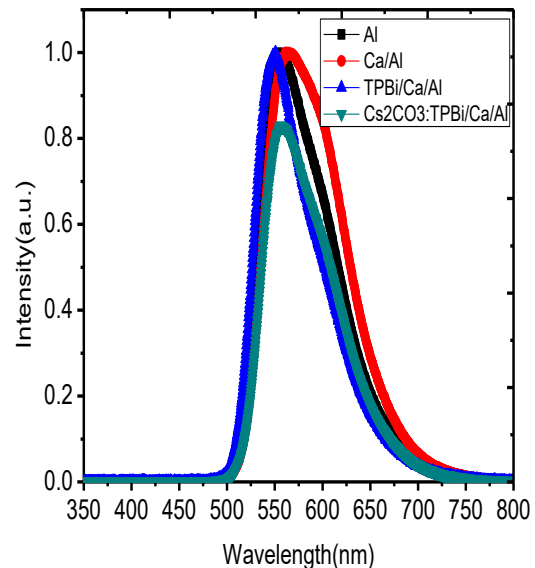


Fig. 5. Normalized EL spectrum of characteristics of Al, Ca/Al TPBi/Ca/Al and $\text{Cs}_2\text{CO}_3\text{:TPBi/Ca/Al}$ as the device cathode

The normalized electroluminescence (EL) as a function of the emission wavelength (nm) of PLEDs with Al, Ca/Al TPBi/Ca/Al and $\text{Cs}_2\text{CO}_3\text{:TPBi/Ca/Al}$ were shown in Fig. 5. The yellow shift could be due to the oxidative-degradation of HY-PPV caused by the Cs_2CO_3 and TPBi on top of it. To assure that whether the spin coated of Cs_2CO_3 and TPBi can generate an oxidative-degradation.

4. Conclusions

In summary, we present multilayered PLEDs by solution processing using Cs_2CO_3 doped TPBi as an n-doped electron transport layer. The device with n-doped ETL were found to achieve significantly enhanced performance. Compared to the control device with undoped TPBi as ETL, the current efficiency of n-doped device is enhanced, and the turn on voltage is reduced significantly. The device has a maximum brightness of 31577 cd/m^2 and current efficiency 6.7 cd/A, which are 23500 cd/m^2 and 5.45 cd/A of the undoped TPBi cathode device respectively. These results demonstrating that the solution processing of n-doped small molecular electron transport layer is a promising strategy for applications in fully solution processed multilayered organic electronic devices.

Acknowledgements

This research was supported by the Academic Research fund of Hoseo University, project # 2014-043.

References

- [1] S. Reineke, F. Linder, G. Schwartz, N. Seidler, K. Walzer, B. Lussem, K. Leo, *Nature* **59**, 234 (2009).
- [2] M. V. MadhavaRao, Y. K. Su, T. S. Huang, C. H. Yeh, M. L. Tu, *Nanoscale Res. Lett.* **4**, 485 (2009).
- [3] M. V. Madhava Rao, Y. K. Su, T. S. Huang, M. L. Tu, S. S. Wu, C. Y. Huang, *J. Electrochem. Soc.* **157**, H832 (2010).
- [4] T. Chiba, Y. J. Pu, M. H. Irasawa, A. Masuhara, H. Sasabe, J. Kido, *ACS Appl. Mater. Interfaces* **4**(11), 6104 (2012).
- [5] M. V. MadhavaRao, T. S. Huang, Y. K. Su, Y. T. Huang, *J. Electrochem. Soc.* **157**, H69 (2010).
- [6] P. W. M. Blom, M. C. J. M. Vissenberg, *Mater. Sci. Eng. R: Reports* **27**, 53 (2000).
- [7] J. H. Kong, G. W. Kim, R. Lampade, G. H. Kim, M. J. Park, H. W. Bae, J. H. Kwon, *Organic Electronics* **21**, 210 (2015).
- [8] M. V. Madhava Rao, Y. K. Su, T. S. Huang, *ECS Solid State Letters* **2**(1), R5-R7 (2013).
- [9] M. V. Madhava Rao, T. S. Huang, Y. K. Su, M. L. Tu, C. Y. Huang, S. S. Wu, *Nano-Micro Letters* **2**(1), 49 (2010).
- [10] W. W. Zhang, Z. X. Wu, X. W. Zhang, S. X. Liang, B. Jiao, X. Hou, *Chin. Sci. Bull.* **56**, 2210 (2011).
- [11] C. Zhong, C. Duan, F. Huang, H. Wu, Y. Cao, *Chem. Mater.* **23**, 326 (2011).
- [12] X. Xu, G. Yu, Y. Liu, D. Zhu, *Display* **27**, 24 (2006).
- [13] F. Huang, H. Wu, Y. Cao, *Chem. Soc. Rev.* **39**(7), 2500 (2010).
- [14] A. P. Kulkarni, C. J. Tonzola, A. Babel, S. A. Jenekhe, *Chem. Mater.* **16**, 4556 (2004).
- [15] S. Ho, S. Liu, Y. Chen, F. So, *J. Photon. Energy* **5**(a), 057611 (2015).
- [16] P. Piromerium, H. Oh, Y. Shen, G. G. Malliaras, J. C. Scott, P. J. Brock, *Appl. Phys. Lett.* **77**, 2403 (2000).
- [17] P. C. Wei, D. D. Zhang, M. Cai, X. Song, Z. Wang, L. Duan, *Organic Electronics* **49**, 242 (2017).
- [18] Q. F. Xu, J. Y. Quyang, Y. Yang, T. Ito, J. Kide, *Appl. Phys. Lett.* **83**, 4695 (2003).
- [19] L. Ma, Z. Xie, J. Liu, J. Yang, Y. Cheng, L. Wang, F. Wang, *Appl. Phys. Lett.* **87**, 163502 (2005).
- [20] J. Huang, Z. Xu, Y. Yang, *Adv. Funct. Mater.* **17**, 1966 (2007).
- [21] Chung-Chin Hsiao, An-En Hsiao, Show-An Chen, *Adv. Mater.* **20**, 1982 (2008).
- [22] T. Earmme, S. A. Jenekhe, *Adv. Funct. Mater.* **22**, 5126 (2012).
- [23] T. Earmme, S. A. Jenekhe, *Appl. Phys. Lett.* **102**, 233305 (2013).
- [24] R. H. Friend, R. W. Gymer, A. B. Holmes, J. H. Burroughes, R. N. Marks, C. Taliani, D. D. C. Bradley, D. A. DosSantos, J. L. Bredas, M. Logdlund, W. R. Salaneck, *Nature* **397**, 121 (1999).
- [25] T. Yamamoto, H. Kajii, Y. Ohmori, *Organic Electronics* **15**(6), 1077 (2014).
- [26] L. Li, Z. Yu, W. Hu, C. H. Chang, Q. Chen, Q. Pei, *Adv. Mater.* **23**, 5563 (2011).
- [27] X. W. Zhang, X. Guo, Y. H. Chen, J. Y. Wang, Z. F. Lei, W. Y. Lai, Q. L. Fan, W. Huang, *J. Lumin.* **161**, 300 (2015).
- [28] Y. Tao, X. Guo, L. Hao, R. Chen, H. Li, Y. Chen, X. Zhang, W. Lai, W. Huang, *Adv. Mater.* **27**, 6939 (2015).
- [29] Q. Zhao, W. Zhang, Z. Fan, J. Li, X. Chen, G. Luo, X. Zhang, *Synth. Met.* **204**, 70 (2015).
- [30] V. Jankus, C. J. Chiang, F. Dias, A. P. Monkman, *Adv. Mater.* **25**, 1455 (2013).

*Corresponding author: madhavamora@yahoo.com
chmoon@hoseo.edu